



## Synthesis of mixed phase anatase-TiO<sub>2</sub>(B) by a simple wet chemical method

Sreenivasan Koliyat Parayil<sup>a</sup>, Harrison S. Kibombo<sup>a</sup>, Luther Mahoney<sup>a</sup>, Chia-Ming Wu<sup>a</sup>,  
Minjoong Yoon<sup>b</sup>, Ranjit T. Koodali<sup>a,\*</sup>

<sup>a</sup> Department of Chemistry, University of South Dakota, Vermillion, SD 57069, USA

<sup>b</sup> Department of Chemistry, Chungnam National University, Daejeon 305-764, South Korea

### ARTICLE INFO

#### Article history:

Received 18 November 2012

Accepted 28 December 2012

Available online 8 January 2013

#### Keywords:

Trititanate nanotube

Urea treatment

Mixed phase anatase-TiO<sub>2</sub>(B)

Solar hydrogen

### ABSTRACT

A photoactive mixed phase, anatase-TiO<sub>2</sub>(B) was synthesized from a mixture of trititanate nanotube and urea at relatively mild conditions. This material exhibited enhanced photocatalytic hydrogen generation under simulated solar irradiation. The enhancement was credited to the presence of mixed phases of anatase and TiO<sub>2</sub>(B) that minimized charge-carrier recombination. The results validate the superior performance of anatase-TiO<sub>2</sub>(B) compared to anatase or TiO<sub>2</sub>(B) alone. Such mixed phase materials may also be applicable for solar assisted degradation of persistent organic pollutants and solar energy conversion devices.

© 2013 Elsevier B.V. All rights reserved.

### 1. Introduction

Trititanate nanotubes (TNT) are inorganic layered materials constituting of titanium oxides [1], which can be tuned to manifest various functionalities. The presence of layered structure provides spatial accommodation of protons or other cationic species and such nanostructures have found relevance in photocatalysis [2], batteries [3], and solar cells [4]. TNT can be transformed to anatase, rutile, TiO<sub>2</sub>(B) or mixed phases [5,6]. However, it is difficult to get photoactive TiO<sub>2</sub>(B)-anatase mixtures under mild experimental conditions. Anatase-TiO<sub>2</sub>(B) mixtures have been prepared by sintering at 810 °C followed by annealing at 600 °C [6,7], using multistep synthesis followed by calcination [5,8], prolonged synthesis times followed by calcination at 400 °C [9] and 600 °C [10], hydrothermal treatment and annealing in air for long duration [11] or hydrothermal treatment followed by calcination at 800 °C [12], tedious method involving layer-by-layer self-assembly [13], or by using surfactants [14]. Therefore, it is highly desirable to design anatase-TiO<sub>2</sub>(B) by simple physico-chemical treatments. The capability of synthesizing anatase-TiO<sub>2</sub>(B) from TNT under relatively mild conditions is lacking in the literature and hence is the focus of this study.

In this work, we prepared mixed anatase-TiO<sub>2</sub>(B) phases from TNT by a simplified method using urea at relatively low reaction temperature [15,16]. Variations in the crystal phases were observed through XRD, Raman, and the performance of the resultant photocatalysts were tested for solar hydrogen generation. This manuscript

is the first report illustrating the preparation of anatase-TiO<sub>2</sub>(B) from TNT by using urea.

### 2. Experimental section

**Preparation of anatase-TiO<sub>2</sub>(B):** TNT was synthesized by a method proposed earlier [17]. For the preparation of anatase-TiO<sub>2</sub>(B), TNT was treated with aqueous urea and the mixture was subjected to heat treatment at 400 °C for 3 h at a heating rate of 3 °C/min and cooled gradually. The powder obtained was washed with deionized water and dried at 100 °C to obtain anatase-TiO<sub>2</sub>(B). Anatase and TiO<sub>2</sub>(B) were prepared for comparison as reported previously [18].

**Characterization:** The materials were characterized by nitrogen physisorption (Quantachrome Nova2200e), powder X-ray diffraction (XRD, Rigaku Ultima IV), Raman (Horiba Jobin Yvon), and diffuse reflectance spectroscopy (DRS, Cary 100 Bio). More detailed characterization techniques are discussed in the **Supplementary section**. Photocatalytic hydrogen evolution reactions were carried out under simulated solar radiation in a quartz reactor as reported previously [19].

### 3. Results and discussion

Fig. 1 shows the XRD pattern of anatase, anatase-TiO<sub>2</sub>(B), and TiO<sub>2</sub>(B). The XRD of TNT is consistent with prior report [17]. Anatase-TiO<sub>2</sub>(B) shows peaks at  $2\theta = 24.90^\circ$ ,  $29.94^\circ$ ,  $43.97^\circ$ ,  $48.1^\circ$ , and  $62.9^\circ$  alluded to  $d_{110}$ ,  $d_{401}$ ,  $d_{003}$ , and  $d_{020}$ ,  $d_{114}$  of TiO<sub>2</sub>(B) (JCPDS, 074-1940). Other peaks observed are characteristic of anatase [20]. The peaks associated with the anatase in anatase-TiO<sub>2</sub>(B) material is prominent than TiO<sub>2</sub>(B) indicating better crystallinity of anatase.

\* Corresponding author. Tel.: +1 605 677 6189; fax: +1 605 677 6397.

E-mail addresses: [Ranjit.Koodali@usd.edu](mailto:Ranjit.Koodali@usd.edu), [ktranjit@gmail.com](mailto:ktranjit@gmail.com) (R.T. Koodali).

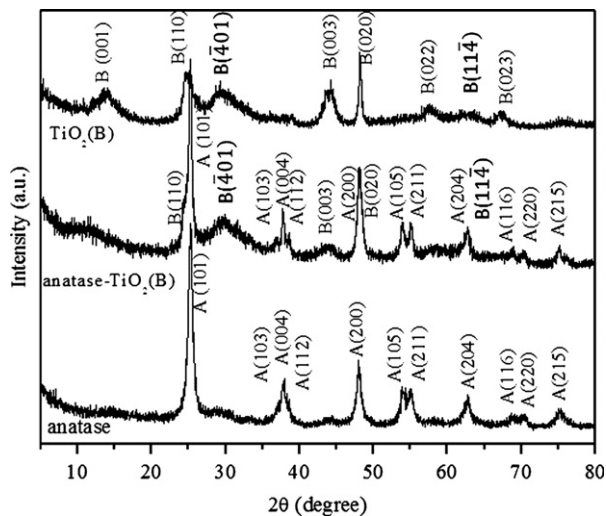


Fig. 1. XRD patterns of anatase,  $\text{TiO}_2(\text{B})$ , and anatase- $\text{TiO}_2(\text{B})$ . A and B refer to anatase and  $\text{TiO}_2(\text{B})$  phase.

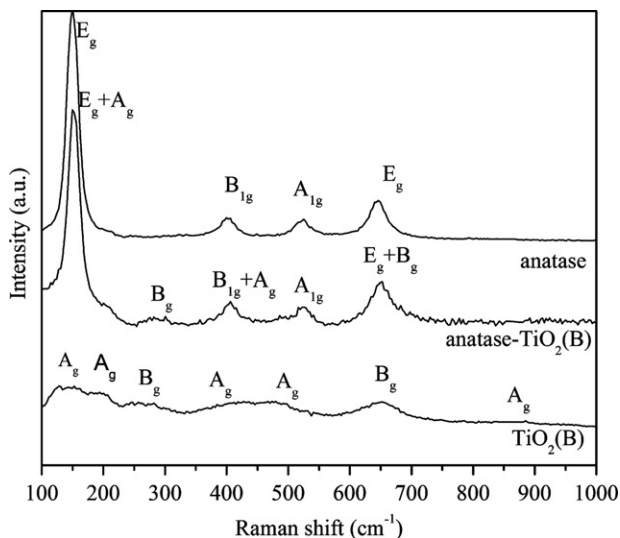


Fig. 2. Raman spectra of anatase,  $\text{TiO}_2(\text{B})$ , and anatase- $\text{TiO}_2(\text{B})$ .

Fig. 2 displays the Raman spectra of anatase, anatase- $\text{TiO}_2(\text{B})$ , and  $\text{TiO}_2(\text{B})$ . The Raman spectra of TNT indicates bands identical to that reported previously [21].

The spectra of anatase- $\text{TiO}_2(\text{B})$  shows a band near  $140\text{ cm}^{-1}$  due to anatase ( $E_g$ ) and  $\text{TiO}_2(\text{B})$  ( $A_g$ ), while the band near  $391\text{ cm}^{-1}$  is due to anatase ( $B_{1g}$ ), and  $\text{TiO}_2(\text{B})$  ( $A_g$ ). The band at  $508\text{ cm}^{-1}$  is due to anatase ( $A_{1g}$ ) and the one at  $637\text{ cm}^{-1}$  is due to anatase ( $E_g$ ), and  $\text{TiO}_2(\text{B})$  ( $B_g$ ). In addition, a subtle shoulder observed at  $190\text{ cm}^{-1}$ , and a low intensity feature at  $266\text{ cm}^{-1}$  in anatase- $\text{TiO}_2(\text{B})$  suggest the presence of the  $\text{TiO}_2(\text{B})$  [20]. These results indicate phase transition of TNT to anatase- $\text{TiO}_2(\text{B})$ . The weak intensity of the Raman peaks preclude the calculation of the percentages of anatase and  $\text{TiO}_2(\text{B})$  in the anatase  $\text{TiO}_2(\text{B})$  material [11].

Based on related works [22–24] we postulate that the preparation of the mixed phases may involve several steps. The first step may be the hydrolysis of urea to form ammonium and isocyanate ions. The ammonium ions can exchange with  $\text{Na}^+$  in TNT and then decompose and escape as ammonia gas. Isocyanate ions form gaseous ammonia and carbon dioxide. Thus, during the heating of TNT with urea, destabilization of TNT occurs followed by nucleation and growth of anatase and  $\text{TiO}_2(\text{B})$  mixed phases. Thus, the

decomposition of urea under *in-situ* conditions favors the formation of highly active mixed phases of anatase and  $\text{TiO}_2(\text{B})$ .

$\text{N}_2$ -sorption isotherm and pore size distribution of the anatase- $\text{TiO}_2(\text{B})$  is shown in Fig. S1, which reveals that the isotherm is of Type IV with H3 hysteresis according to IUPAC [25]. A broader range of pores is suggested for anatase- $\text{TiO}_2(\text{B})$ ; most of the pores are centered around 36 nm. The isotherm does not level off at high relative pressures indicating the presence of macropores, i.e. intra-particle pores. The physico-chemical data of the materials prepared in this study are shown in Table 1.

A decrease in surface area is noted for anatase- $\text{TiO}_2(\text{B})$ . This may be due to phase transition, which led to the agglomeration and partial deformation of nanotube thus limiting  $\text{N}_2$  access to the pores. This is reiterated by the reduction in pore volume of anatase- $\text{TiO}_2(\text{B})$ .

The DRS of TNT,  $\text{TiO}_2(\text{B})$ , anatase, and anatase- $\text{TiO}_2(\text{B})$ , are shown in Fig. S2. The Kubelka–Munk estimation of band gap ( $E_g$ ) for these materials is shown in Table 1.

The morphological features of samples were investigated by TEM as shown in Fig. S3. The images validate the formation of the tubular morphology for TNT and the presence some tubes for anatase- $\text{TiO}_2(\text{B})$ . XPS analysis indicates the absence of nitrogen in anatase- $\text{TiO}_2(\text{B})$  as shown in Fig. S4. In addition, elemental analyses also indicate the absence of nitrogen.

Table 1

Textural and photocatalytic properties of anatase- $\text{TiO}_2(\text{B})$  and related materials.

Materials	Surface area <sup>a</sup> ( $\text{m}^2/\text{g}$ )	Pore volume ( $\text{cm}^3/\text{g}$ )	BJH pore diameter <sup>b</sup> (nm)	Band gap ( $E_g$ ) (eV)	$\text{TiO}_2(\text{B})$ : Anatase <sup>c</sup> (%)	$\text{H}_2$ evolution <sup>d</sup> ( $\mu\text{mol g}^{-1}$ )
TNT	126	0.51	2.4	3.46	0	30
Anatase- $\text{TiO}_2(\text{B})$	76	0.27	2.4	3.20	52:48	240
Anatase	61	0.14	3.8	3.11	0:100	110
$\text{TiO}_2(\text{B})$	421	0.47	2.2	3.25	100:0	4

<sup>a</sup> Surface area determined by applying Brunauer–Emmett–Teller (BET) equation to a relative pressure ( $P/P_0$ ) range of 0.05–0.30 of the adsorption isotherm.

<sup>b</sup> Pore diameter is calculated from the Barrett–Joyner–Halenda (BJH) equation using the desorption isotherm.

<sup>c</sup> Determined by quantitative analysis using the Reference Intensity Ratio (RIR) method of the PDXL software (the error is estimated to be 5%).

<sup>d</sup> Photocatalytic efficiencies after 4 h under solar simulated irradiation conditions.

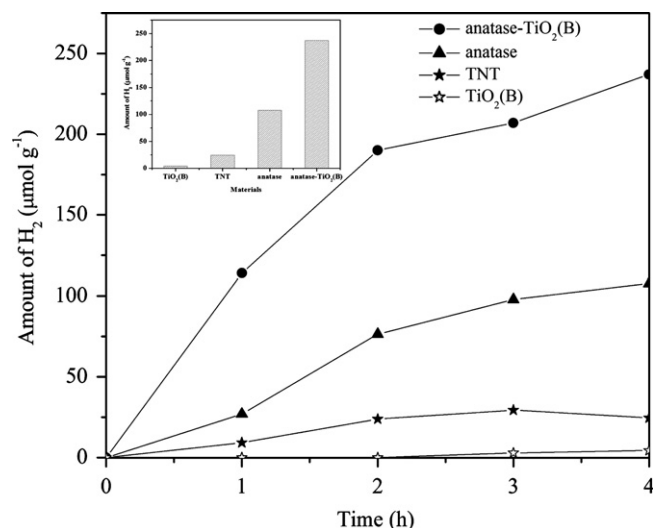


Fig. 3.  $\text{H}_2$  evolution by TNT,  $\text{TiO}_2(\text{B})$ , anatase, and anatase- $\text{TiO}_2(\text{B})$ . The value recorded after 4 h of irradiation on  $\text{TiO}_2(\text{B})$ , TNT, anatase, and anatase- $\text{TiO}_2(\text{B})$  are shown in inset.

Fig. 3 shows the H<sub>2</sub> evolution plot of the synthesized materials. TNT evolves only 30 μmol g<sup>-1</sup> of H<sub>2</sub> of catalyst after 4 h of irradiation indicating low activity [26,27]. TiO<sub>2</sub>(B), anatase, and anatase-TiO<sub>2</sub>(B) produce 4, 110, and 240 μmol g<sup>-1</sup> of H<sub>2</sub>, respectively, suggesting that the enhanced activity of anatase-TiO<sub>2</sub>(B) is due to effective charge separation of electron–hole pairs due to differences in conduction band-gap edges of anatase and TiO<sub>2</sub>(B) in the mixed phase material that promote vectorial transfer of electrons from one phase to another [5,6]. In addition the high crystallinity of anatase phase in anatase-TiO<sub>2</sub>(B), and effective utilization of solar radiation (due to slightly lower E<sub>g</sub>) may also contribute to the higher activity of anatase-TiO<sub>2</sub>(B).

Photoluminescence experiments were conducted for anatase-TiO<sub>2</sub>(B), anatase, and TiO<sub>2</sub>(B). Anatase-TiO<sub>2</sub>(B) shows lower emission indicating minimization of the charge carrier recombination, which support the photocatalytic results.

#### 4. Conclusions

The synthesis of anatase-TiO<sub>2</sub>(B) crystal phase by the thermal treatment of TNT and urea solution was investigated. The materials exhibited improved photocatalytic activity due to formation of mixed phases of anatase-TiO<sub>2</sub>(B) that minimize electron–hole recombination. The high activity of anatase-TiO<sub>2</sub>(B) is attributed to high crystallinity of anatase phase in anatase-TiO<sub>2</sub>(B), lower band gap energy and most importantly due to minimized electron–hole recombination. The mild conditions of thermal treatment demonstrated in this study opens new avenues for preparation of such mixed phase materials for solar energy conversion applications. More detailed studies related to the phase transitions of TNT under controlled treatment of urea are in progress.

#### Acknowledgment

This work was supported by DE-EE-0000270, NSF-CHE-0840507, NSF-CHE-0722632, and NSF-EPSC-0903804. Prof. M. Yoon thanks the National Research Foundation of Korea (NRF 2010-0795) for support. We are thankful to Dr. C.Y. Jiang for Raman and Dr. C. Lin for TEM studies.

#### Appendix A. Supporting information

Supplementary data associated with this article can be found in the online version at <http://dx.doi.org/10.1016/j.matlet.2012.12.109>.

#### References

- [1] Li N, Zhang L, Chen Y, Fang M, Zhang J, Wang H. *Adv Funct Mater* 2012;22: 835–41.
- [2] Xiong L, Sun W, Yang Y, Chen C, Ni J. *J Colloid Interface Sci* 2011;356:211–6.
- [3] Wu HB, Lou XW, Hng HH. *Chem Eur J* 2012;18:2094–9.
- [4] Zhao L, Yu J, Fan J, Zhai P, Wang S. *Electrochem Commun* 2009;11:2052–5.
- [5] Yang D, Liu H, Zheng Z, Yuan Y, Zhao J-c, Waclawik ER, et al. *J Am Chem Soc* 2009;131:17885–93.
- [6] Li W, Liu C, Zhou Y, Bai Y, Feng X, Yang Z, et al. *J Phys Chem C* 2008;112: 20539–45.
- [7] Li W, Bai Y, Liu C, Yang Z, Feng X, Lu X, et al. *Environ Sci Technol* 2009;43:5423–8.
- [8] Liu B, Khare A, Aydil ES. *ACS Appl Mater Interfaces* 2011;3:4444–50.
- [9] Yang Z, Du G, Guo Z, Yu X, Chen Z, Guo T, et al. *Electrochem Commun* 2011;13:46–9.
- [10] Fu N, Wu Y, Jin Z, Lu G. *Langmuir* 2009;26:447–55.
- [11] Beuviel T, Richard-Plouet M, Brohan L. *J Phys Chem C* 2009;113:13703–6.
- [12] Zhou W, Gai L, Hu P, Cui J, Liu X, Wang D, et al. *Cryst Eng Comm* 2011;13:6643–9.
- [13] Pan K, Dong Y, Zhou W, Wang G, Pan Q, Yuan Y, et al. *Electrochim Acta* 2013;88:263–9.
- [14] Hongo T, Yamazaki A. *Microporous Mesoporous Mater* 2011;142:316–21.
- [15] Mapa M, Sivaranjani K, Bhang DS, Saha B, Chakraborty P, Viswanath AK, et al. *Chem Mater* 2009;22:565–78.
- [16] Sivaranjani K, Gopinath CS. *J Mater Chem* 2011;21:2639–47.
- [17] Kasuga T, Hiramoto M, Hoson A, Sekino T, Niihara K. *Langmuir* 1998;14: 3160–3.
- [18] Kiatkittipong K, Scott J, Amal R. *ACS Appl Mater Interfaces* 2011;3:3988–96.
- [19] Parayil SK, Kibombo HS, Wu C-M, Peng R, Baltrusaitis J, Koodali RT. *Int J Hydrogen Energy* 2012;37:8257–67.
- [20] D'Elia D, Beauger C, Hochepeid J-F, Rigacci A, Berger M-H, Keller N, et al. *Int J Hydrogen Energy* 2011;36:14360–73.
- [21] Qamar M, Yoon CR, Oh HJ, Kim DH, Jho JH, Lee KS, et al. *Nanotechnology* 2006;17:5922–9.
- [22] Chang J-C, Tsai W-J, Chiu T-C, Liu C-W, Chao J-H, Lin C-H. *J Mater Chem* 2011;21:4605–14.
- [23] Chen Q, Zhou W, Du GH, Peng LM. *Adv Mater* 2002;14:1208–11.
- [24] Liu H, Waclawik ER, Zheng Z, Yang D, Ke X, Zhu H, et al. *J Phys Chem C* 2010;114:11430–4.
- [25] Kruk M, Jaroniec M. *Chem Mater* 2001;13:3169–83.
- [26] Sylwia M. *Catal Today* 2010;156:198–207.
- [27] Inagaki M, Kondo N, Nonaka R, Ito E, Toyoda M, Sogabe K, et al. *J Hazard Mater* 2009;161:1514–21.